Iranian Journal of Medical Physics

ijmp.mums.ac.ir

Quantitative Dynamic Susceptibility Contrast MRI for Non-Invasive Glioma Grading: The Role of rCBV and rCBF

Fateme Shahedi [1], Hoda Zare [2*]

1. Department of Radiology Technology, School of Paramedical Sciences, Mashhad University of Medical Sciences, Mashhad, Iran
2. Medical Physics Research Center, Basic Sciences Research Institute, Mashhad University of Medical Sciences, Mashhad, Iran

ARTICLE INFO

Article type:
Original Paper

Keywords:
Magnetic Resonance Imaging
Dynamic Susceptibility Contrast
Glioma

ABSTRACT

Introduction: Accurate preoperative grading of gliomas is essential for personalized treatment planning; however, conventional MRI often fails to reliably differentiate low-grade gliomas from high-grade gliomas due to overlapping imaging characteristics. Dynamic susceptibility contrast (DSC) MRI provides quantitative perfusion biomarkers that more directly reflect tumor vascularity and biological aggressiveness. This study aimed to evaluate the diagnostic utility of relative cerebral blood volume (rCBV) and relative cerebral blood flow (rCBF) for non-invasive glioma grading and to characterize regional perfusion patterns across distinct tumor compartments.

Material and Methods: Thirty patients with histopathologically confirmed gliomas underwent preoperative structural and DSC-MRI. Quantitative rCBV and rCBF maps were generated using standardized acquisition and post-processing protocols. Regions of interest were placed within the contrast-enhancing tumor, peritumoral edema, tumor core, and contralateral normal-appearing white matter. Perfusion metrics were compared across tumor subregions and between glioma grades. Diagnostic performance was assessed using receiver operating characteristic (ROC) analysis.

Results: High-grade gliomas exhibited significantly higher rCBV and rCBF than low-grade gliomas ($p < 0.05$). In high-grade gliomas, the enhancing region exhibited markedly increased perfusion relative to the contralateral hemisphere, whereas the tumor core showed significantly reduced values. No significant perfusion differences were observed within the edema region. ROC analysis demonstrated strong diagnostic performance for both biomarkers, with rCBV achieving the best diagnostic performance (AUC=0.941, 95% CI: 0.821, 0.992, $p<0.05$).

Conclusion: Quantitative rCBV and rCBF show promising potential as biologically meaningful indicators of glioma grade, reflecting vascularity-related tumor biology. These metrics enhance non-invasive tumor characterization and may assist in optimizing surgical planning and individualized therapeutic strategies.

► *Please cite this article as:*
Shahedi F, Zare H. Quantitative Dynamic Susceptibility Contrast MRI for Non-Invasive Glioma Grading: The Role of rCBV and rCBF. Iran J Med Phys 2026; 23 (2): 124-131. 10.22038/ijmp.2026.95343.2690.

Introduction

Gliomas are the most common primary tumors of the central nervous system and represent a heterogeneous group of neoplasms with diverse biological behavior and clinical outcomes. According to the World Health Organization (WHO) classification, they are categorized into low-grade and high-grade tumors based on histopathological and molecular features [1]. High-grade gliomas show more aggressive growth, increased angiogenesis, and poorer prognosis than low-grade tumors [2]. Therefore, accurate tumor grading is crucial for patient management, as treatment strategies and prognosis strongly depend on tumor grade. Histopathological analysis of biopsy is the gold standard for glioma grading, allowing direct evaluation of cellularity, mitosis, necrosis, and microvascular proliferation [3]. However, biopsy is invasive, carries risks, and may not fully represent the entire tumor due to its heterogeneity, potentially leading to misclassification [4]. It can also be challenging or unsafe in deep or eloquent brain regions [5]. Furthermore, the optimal extent of surgical resection is influenced by tumor grade, with more extensive resection improving survival in diffuse low-grade gliomas [6]. These limitations highlight the need for reliable non-invasive imaging biomarkers that can predict tumor grade preoperatively. Magnetic resonance imaging (MRI) is the standard modality for brain tumor evaluation because of its excellent soft-tissue contrast and multiparametric capability. While conventional MRI sequences (T1-weighted, T2-weighted, and fluid-attenuated inversion recovery) offer valuable anatomical information, they are often insufficient for distinguishing low-grade from high-grade gliomas due to overlapping imaging features [7]. As a result, advanced MRI techniques have gained interest for providing functional and physiological insights into the tumor microenvironment. Perfusion-weighted MRI is a key non-invasive method for evaluating tumor vascularity

*Corresponding Author: Tel: +98-5138002321; Fax: +98-5138002320; Email: Zareh@mums.ac.ir

and hemodynamics. Dynamic susceptibility contrast (DSC) MRI, in particular, allows quantification of hemodynamic parameters linked to angiogenesis and microvascular density, with relative cerebral blood volume (rCBV) and relative cerebral blood flow (rCBF) being the most commonly used metrics [8]. High-grade gliomas typically exhibit increased vascular proliferation, and previous studies suggest that perfusion metrics may serve as imaging biomarkers for tumor grading by reflecting underlying vascular physiology [9]. However, variability in imaging protocols, analysis methods, and patient populations has produced inconsistent findings, highlighting the need for further investigation. Furthermore, previous research has often evaluated tumors as a whole or focused on isolated regions, thereby overlooking the spatial heterogeneity of tumors. Furthermore, no study has comprehensively evaluated and compared these perfusion parameters across the three distinct tumor compartments simultaneously within the same cohort. Non-invasive biomarkers capable of reliably predicting glioma grade have significant clinical value, helping to guide treatment decisions, improve biopsy targeting, and support monitoring of disease progression. Therefore, the aim of the present study was to evaluate glioma vascular characteristics using quantitative DSC perfusion imaging biomarkers, specifically rCBV and rCBF within different regions of the tumor, and to assess the potential of these biomarkers for the non-invasive differentiation of low-grade and high-grade gliomas.

Materials and Methods

Patient Selection

Patients with a radiological suspicion of glioma who had not received any prior treatment were prospectively recruited between May 2024 and February 2025. All subjects underwent preoperative MRI imaging within two weeks preceding surgical tumor removal. The final tumor grading was established through histopathological assessment and molecular testing in accordance with the World Health Organization (WHO) classification criteria. Each participant provided written informed consent before inclusion in the study.

MRI Acquisition Protocol

All MRI examinations were performed using a 1.5-T Philips Ingenia system (Philips Medical Systems, Best, Netherlands) equipped with a standard head coil. The imaging protocol included conventional structural sequences; T1-weighted imaging, T2-weighted imaging, and fluid-attenuated inversion recovery (FLAIR) followed by dynamic susceptibility contrast (DSC) T2*-weighted perfusion imaging* and post-contrast T1-weighted imaging. DSC perfusion imaging was acquired using a single-shot gradient-echo echo-planar imaging (GRE-EPI) sequence. The acquisition parameters were as follows: repetition time (TR) = 3742 ms, echo time (TE) = 47 ms, flip angle = 90°, field of view = 220 × 220 mm², and 33 interleaved slices with a slice thickness of 4 mm and no interslice gap. A total of 50 dynamic volumes were acquired during the perfusion experiment. A gadoterate meglumine (Dotarem, Guerbet) was administered intravenously at a dose of 0.2 mL/kg, followed by a 20 mL saline flush to ensure rapid delivery of the contrast bolus. Prior to DSC acquisition, a preload dose 0.05 mmol/kg of gadolinium-based contrast agent was administered to reduce T1 leakage effects associated with blood brain barrier disruption in tumors. The dynamic perfusion data were subsequently processed using Neuroperfusion software (Philips Healthcare, Best, The Netherlands) on the manufacturer's workstation. The perfusion dataset consisted of 50 dynamic volumes, each containing 33 brain slices. Because the images were acquired over multiple time points, motion correction was first applied to minimize the effects of patient movement during dynamic acquisition. During the first pass of the contrast agent through the cerebral vasculature, susceptibility induced signal loss on T2*-weighted images was measured to estimate changes in contrast agent concentration within each voxel, as illustrated in Figure 1. To minimize T1 leakage effects caused by blood–brain barrier disruption, in addition to administering a preload dose of gadolinium contrast agent, leakage correction was also performed using the Boxerman method [10]. In this approach, voxels with minimal leakage effects were identified based on the recovery of the post-bolus signal toward baseline.

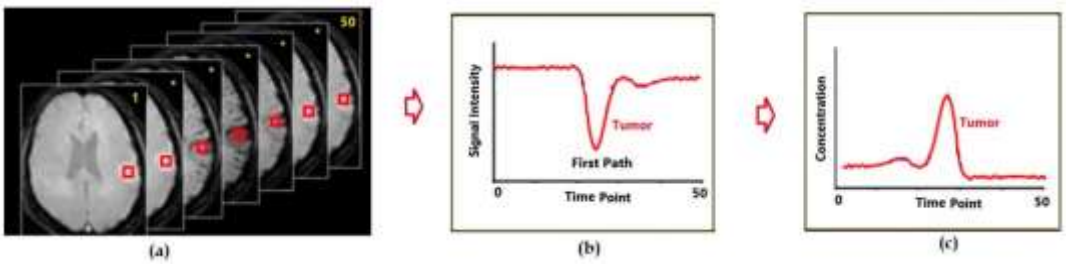

Figure 1. Acquisition of DSC images in 50 dynamic volumes at different time points (a). Determination of the signal intensity–time curve for each voxel and its corresponding voxels across all 50 volumes (b), Conversion of the signal intensity–time curve of each voxel into a contrast agent concentration–time curve (c).

The average concentration–time curve from these reference voxels was then used as a model of the first-pass response, and voxel-wise fitting was performed to estimate leakage correction coefficients, resulting in leakage-corrected perfusion maps. Subsequently, the signal–time curves obtained from the dynamic images were converted into contrast concentration–time curves for each voxel based on the established relationship between T2* signal intensity and contrast agent concentration [11]. Since estimation of perfusion parameters requires characterization of the contrast agent input to the cerebral circulation, a branch of the middle cerebral artery was manually selected based on high signal intensity and early bolus arrival characteristics, after which the software automatically calclated the arterial input function (AIF) from the selected vessel. Perfusion parameters were then calculated using singular value decomposition (SVD)-based deconvolution analysis. Finally, relative cerebral blood volume (rCBV) and relative cerebral blood flow (rCBF) maps were generated by normalizing perfusion values measured in the solid tumor component to those obtained from contralateral normal-appearing white matter.

Image Registration

Image registration was performed using the Advanced Normalization Tools (ANTs; University of Pennsylvania, Philadelphia, PA, USA) software package, which provides high-accuracy affine and deformable image alignment. All skull-stripped perfusion maps (rCBV and rCBF) and structural images were co-registered to the corresponding post-contrast skull-stripped T1-weighted image to align corresponding brain voxels across images. Brain extraction was also performed using FSL brain extraction tool (BET; FMRIB Software Library, University of Oxford, Oxford, UK).

Region of Interest (ROI) Placement

Two blinded neuroradiologists independently delineated ROIs on the slice showing the largest cross-sectional tumor using ITK-SNAP (version 3.8), and the segmentations were subsequently cross-checked for consistency. In high-grade tumors, three distinct regions of interest (ROIs), including contrast-enhancing tumor, peritumoral edema, and tumor core (necrotic core) were defined. The contrast-enhancing region identified on post-contrast T1-weighted images to include the solid enhancing portion of the lesion while avoiding obvious necrotic, cystic, and hemorrhagic structures. Peritumoral edema was delineated on FLAIR images, and necrotic tumor core were separately marked as low-signal non-enhancing areas within the enhancing tumor margins. In contrast, because low-grade tumors typically lack contrast enhancement and necrotic components, ROI delineation in these lesions was limited to the solid tumor region corresponding to the hyperintense abnormality on T2-weighted or FLAIR images. Therefore, for comparative analysis between the two groups, perfusion parameters were evaluated in the solid tumor region. To evaluate the relative changes in perfusion parameters compared with normal brain tissue, a corresponding region of interest (ROI) with equal size was placed in the contralateral normal-appearing hemisphere for each ROI separately. Inter-observer agreement was assessed using the intraclass correlation coefficient (ICC), and discrepancies were resolved by consensus.

Statistical Analysis

All statistical analyses were conducted using SPSS software version 26.0 (IBM Corp., Armonk, NY, USA). Data distribution was evaluated with the Shapiro–Wilk test. Differences between tumor regions and contralateral reference areas were analyzed using paired t-tests for normally distributed variables or the Wilcoxon signed-rank test for non-parametric data. Comparisons between low-grade and high-grade gliomas were performed using independent samples t-tests for normally or the Mann–Whitney U test for non-normally distributed variables. Normally distributed data were expressed as mean ± standard deviation (SD), whereas non-normally distributed data were reported as median and interquartile range (IQR). A receiver operating characteristic (ROC) analysis was conducted to quantify the diagnostic performance of the perfusion parameters. The area under the curve (AUC), sensitivity, specificity, and Youden index were calculated from the ROC analysis. The optimal cutoff values for rCBV and rCBF were determined as the threshold values that maximized the Youden index. Bonferroni correction was applied to adjust for multiple comparisons. A p-value < 0.05 was considered statistically significant after Bonferroni correction.

Results

Patient Characteristics

A total of thirty-five patients were screened for eligibility. Following exclusions due to non-glioma histopathology (n = 4), and absence of tissue diagnosis (n = 1), 30 patients with definitive histopathological confirmation of glioma were included in the final analysis. Demographics, clinical, radiological, and histopathological characteristics of patients are detailed in Table 1.

Inter-observer Variability

Inter-observer agreement for ROI-based perfusion measurements is presented in Table 2.

Inter-observer reproducibility of ROI measurements was good across all regions. The ICC values ranged from 0.82 to 0.87 for rCBV and from 0.81 to 0.86 for rCBF across the evaluated ROI types.

Comparison of rCBV and rCBF Maps Across Glioma Subregions Versus Contralateral Hemisphere

Perfusion measurements were successfully obtained in all patients. Table 3 presents the comparison of rCBV and rCBF values between the tumor subregions and the corresponding contralateral normal-appearing hemisphere.

Table 1. Demographic, clinical, radiological, and histopathological characteristics of patients with low-grade and high-grade gliomas included in the study.

Characteristic		Overall	Low-Grade Glioma	High-Grade Glioma
Age, years		48.50±13.54	45.91±6.11	52.61±12.23
Sex (Male/Female)		17(56.7%)/13 (43.3%)	7 (58.3%)/5 (41.7%)	10 (55.6%)/8 (44.4%)
WHO Grade II		12 (40%)	12 (100%)	-
WHO Grade III		3 (100 %)	-	3 (16.7%)
WHO Grade IV		15(50%)	-	15 (83.3%)
Contrast enhancement		18 (60%)	0 (0%)	18(100%)
Surgical resection		26 (86.7%)	9 (75%)	17 (94.4%)
Stereotactic biopsy		4 (13.3%)	3 (25%)	1 (5.6%)
MRI-to-surgery interval ≤ 2 weeks		30 (100%)	12 (100%)	18 (100%)
Histopathological subtype	Astrocytoma	8 (26.7%)	8 (66.7%)	0 (0%)
	Oligodendroglioma	4 (13.3%)	4 (33.3%)	0 (0%)
	Anaplastic astrocytoma	9 (50%)	0 (0%)	9 (50%)
	Glioblastoma	9 (30%)	0 (0%)	9 (50%)
Tumor location	Frontal lobe	15 (50.0%)	7 (58.3%)	8 (44.4%)
	Temporal lobe	8 (26.7%)	3 (25%)	5 (27.8%)
	Parietal lobe	5 (16.7%)	2 (16.7%)	3 (16.7%)
	Occipital lobe	2 (6.7%)	0 (0%)	2 (11.1%)

Table 2. Inter-observer agreement for perfusion measurements across different regions of interest (ROIs).

Region of Interest	ICC rCBV, 95% confidence interval	ICC rCBF, 95% confidence interval
Tumor Core	0.86, (0.72–0.94)	0.83, (0.69–0.93)
Enhancement	0.87, (0.74–0.95)	0.85, (0.71–0.94)
Edema	0.82, (0.64–0.92)	0.81, (0.62–0.91)
Contralateral normal white matter	0.85, (0.76–0.95)	0.86, (0.73–0.94)

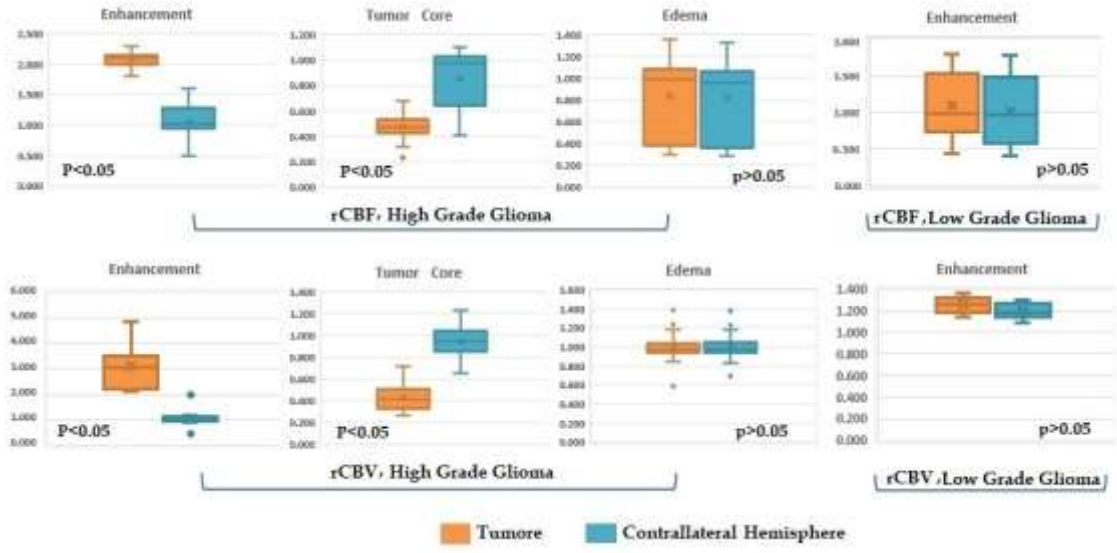

Figure 2. Comparison of DSC-derived perfusion parameters between tumor regions and the corresponding contralateral hemisphere in low-grade and high-grade glioma

Comparison of perfusion parameters between tumor regions and the corresponding contralateral hemisphere in low-grade and high-grade glioma is also illustrated using box plots in Figure 2.

As illustrated in Table 3 and Figure 2, in low-grade gliomas, rCBV and rCBF values in the enhancing region showed no significant differences compared with the contralateral hemisphere ($p>0.05$). In contrast, high-grade gliomas demonstrated markedly higher rCBV and rCBF values in the enhancing region, while the tumor core exhibited significantly lower perfusion metrics compared to the contralateral hemisphere. No significant perfusion differences were observed within the edema region ($p>0.05$).

Table 3. Quantitative comparison of rCBV and rCBF values in enhancing, edema, and tumor core regions versus the contralateral hemisphere in low- and high-grade gliomas.

Perfusion Parameter	Region	Low-grade glioma	Contralateral Hemisphere	Statistical test	P-Value (Bonferroni corrected)
rCBV	Enhancement	1.255±0.702	1.093±0.070	Paired t-tests	0.584
rCBF	Enhancement	1.081±0.451	1.010±0.472	Paired t-tests	0.928
High-grade glioma			Contralateral Hemisphere		
rCBV	Enhancement	3.064±1.304	1.051±0.156	Wilcoxon signed-rank test	<0.001
	Edema	0.993±0.164	1.003±0.151	Paired t-tests	>0.99
	Tumor core	0.402±0.109	0.945±0.162	Paired t-tests	0.024
rCBF	Enhancement	2.088±0.110	1.053±0.314	Paired t-tests	<0.001
	Edema	0.973±0.705	0.963±0.702	Wilcoxon signed-rank test	>0.99
	Tumor core	0.475±0.106	0.972±0.389	Wilcoxon signed-rank test	<0.001

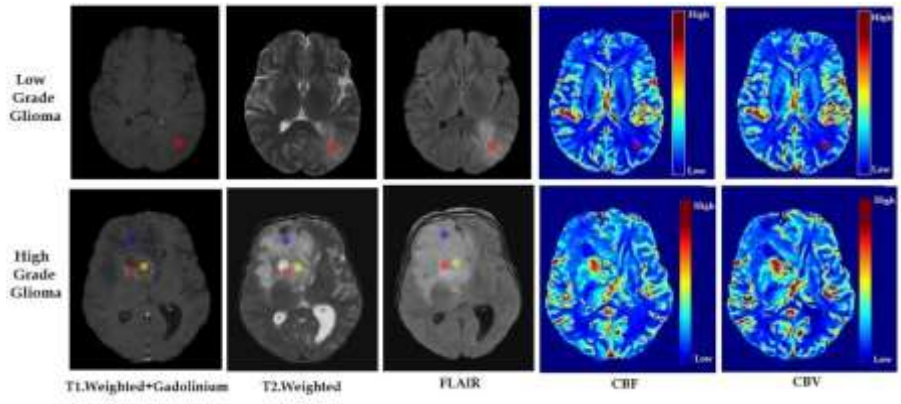

Figure 3. MR images of glioma patients. ROIs were placed on contrast enhancement (red), tumor core (yellow) and peritumoral edema (blue) regions of high-grade tumor and contrast enhancement region of low-grade tumor.

Table 4. Comparison of DSC-derived perfusion parameters in the enhancement region of low-grade gliomas and high-grade gliomas

Perfusion Parameter	Region	Low-grade glioma	High-grade glioma	Statistical test	P-Value (Bonferroni corrected)
rCBV	Enhancement	1.260±0.133	3.064±1.304	Mann–Whitney U test	<0.001
rCBF	Enhancement	1.084±0.451	2.088±0.110	Independent t-test	<0.001

Table 5. Diagnostic performance of perfusion parameters for glioma grading based on receiver operating characteristic (ROC) analysis.

Parameter		Optimal cutoff (Threshold)	Sensitivity, 95% Confidence interval	Specificity, 95% Confidence interval	Youden Index	AUC, 95% Confidence interval	P-Value
rCBF	Low-grade vs high-grade gliomas	1.213	0.912 (0.698, 0.979)	0.874 (0.613, 0.983)	0.786	0.913(0.763, 0.969)	<0.001
rCBV	Low-grade vs high-grade gliomas	1.741	0.930 (0.676, 0.991)	0.892 (0.629, 0.981)	0.822	0.941(0.821, 0.992)	<0.001

The rCBV and rCBF maps of low-grade and high-grade gliomas and the delineated ROIs at various tumor regions is also illustrated in Figure 3.

As shown in Figure 3, high-grade gliomas exhibited significantly higher rCBV and rCBF compared with low-grade gliomas ($p < 0.05$).

Comparison of Perfusion Parameters: High-Grade Versus Low-Grade Gliomas

The results of the comparison of perfusion parameters in the enhancement region between low-grade gliomas and high-grade gliomas are presented in Table 4.

As illustrated in Table 4, the rCBV and rCBF values within the enhancement region were significantly higher in high-grade gliomas compared with low-grade gliomas ($P < 0.001$),

Diagnostic Performance Based on ROC Analysis

The diagnostic performance of perfusion parameters for glioma grading is presented in Table 5.

ROC analysis supported DSC-derived perfusion parameters as useful biomarkers for differentiating low-grade from high-grade gliomas. However, rCBV performed slightly better than rCBF, resulting in an AUC of 0.941 (95% CI: 0.821, 0.992), a sensitivity of 0.930

(95% CI: 0.676, 0.991) and a specificity of 0.892 (95% CI: 0.629, 0.981) .

Discussion

In this study, we evaluated the diagnostic performance of quantitative DSC-MRI biomarkers, particularly rCBV and rCBF, for the non-invasive grading of gliomas. Quantitative perfusion assessment may overcome a key limitation of conventional MRI, namely the imperfect relationship between contrast enhancement and tumor grade. While contrast enhancement reflects blood–brain barrier disruption, it does not always correspond to tumor aggressiveness, as some high-grade gliomas show minimal enhancement and certain low-grade tumors may demonstrate atypical enhancement patterns [12, 13]. According to the results presented in Table 4, rCBV and rCBF values were significantly higher in high-grade gliomas than in low-grade gliomas. These findings are consistent with previous studies demonstrating that increased perfusion correlates with higher glioma grade and microvascular proliferation [14, 15, 16]. Biologically, high-grade gliomas are characterized by endothelial proliferation, abnormal neoangiogenesis, and increased vascular permeability, which contribute to elevated rCBV and rCBF values [17]. Conversely, low-grade gliomas generally exhibit lower microvascular density and less pronounced angiogenic activity [18]. Previous studies have also reported rCBV values below 2 (rCBV<2) in low-grade gliomas [19, 20, 21]. Additionally, the literature indicates that among low-grade gliomas, oligodendrogliomas may demonstrate relatively higher perfusion values, possibly due to larger vessel caliber and their frequent cortical location [18, 22]. Perfusion analysis across different tumor compartments provides further insight into the glioma microenvironment. In this study, perfusion parameters showed distinct patterns in high-grade glioma subregions compared with the contralateral normal hemisphere. The high cellular proliferation and metabolic demand of high-grade gliomas increase oxygen and nutrient requirements, promoting the upregulation of pro-angiogenic factors and subsequently enhancing angiogenesis, which leads to elevated perfusion values in the enhancing tumor component [23]. Previous studies have also reported markedly higher perfusion in enhancing regions of high-grade gliomas relative to the contralateral hemisphere [16, 24, 25]. However, no significant differences were observed between perfusion parameters of low-grade gliomas and contralateral normal tissue, likely reflecting the absence of substantial vascular alterations in these tumors [18]. Interestingly, the peritumoral edema region in high-grade gliomas showed no significant perfusion differences compared to the contralateral hemisphere. Nevertheless, other studies have suggested that increased perfusion within peritumoral edema may indicate tumor cell infiltration in some gliomas, whereas certain high-grade subtypes may lack infiltrative edema [26, 27]. Differentiating vasogenic from infiltrative edema remains important for preoperative planning, and perfusion imaging has been proposed as a useful tool for this purpose [26, 28]. Additionally, perfusion values within the tumor core were lower than those in the contralateral hemisphere, consistent with findings of Senturk et al [29]. This reduction may result from rapid tumor growth and disorganized vascular architecture, which can lead to inadequate perfusion in central tumor regions and contribute to hypoperfusion and further emphasizing the heterogeneous vascular profile of high-grade gliomas [30]. ROC analysis further demonstrated that DSC-derived perfusion parameters can reliably differentiate glioma grades, supporting their value as imaging biomarkers reflecting tumor vascularity and biological aggressiveness. Despite these promising findings, this study has several limitations, including a relatively small sample size and a single-center design, which may limit the generalizability of the results. Therefore, the results should be considered exploratory and require validation in larger, multicenter cohorts to establish robust clinical thresholds. In addition, tumor grading in this cohort was based on classical histopathology rather than the integrated molecular classification recommended by the WHO 2021 criteria. The lack of molecular data, including IDH mutation status and 1p/19q codeletion, prevented correlation of DSC-derived hemodynamic parameters with glioma molecular subtypes, which represents an important limitation of this study. Furthermore, multiparametric imaging approaches, such as the combination of DSC with ASL and radiomics, may help further validate and improve non-invasive glioma characterization in future studies.

Conclusion

Quantitative rCBV and rCBF may serve as promising perfusion biomarkers for non-invasive glioma grading. These perfusion-derived biomarkers reflect underlying vascularity-related tumor biology and offer valuable diagnostic information beyond conventional structural MRI. This kind of analysis can provide relevant diagnostic information in a non-invasive manner and its clinical utility may extend to optimize surgical planning, and guide personalized therapeutic strategies with clinical risk stratification.

Acknowledgment

This research is a part of a PhD thesis and has been funded by the vice chancellor for research of Mashhad University of Medical Science (Grant No. 4020997).

References

1. Antonelli M, Poliani PL. Adult type diffuse gliomas in the new 2021 WHO Classification. Pathologica. 2022;114(6):397.
2. Nowacka A, Śniegocki M, Smuczyński W, Bożiłow D, Ziółkowska E. Angiogenesis in glioblastoma—treatment approaches. Cells. 2025;14(6):407.
3. Ahmed R, Oborski MJ, Hwang M, Lieberman FS, Mountz JM. Malignant gliomas: current perspectives

in diagnosis, treatment, and early response assessment using advanced quantitative imaging methods. Cancer management and research. 2014:149-70.
4. Setyawan NH, Choridah L, Nugroho HA, Malueka RG, Dwianingsih EK. Beyond invasive biopsies: using VASARI MRI features to predict grade and molecular parameters in gliomas. Cancer Imaging. 2024;24(1):3.
5. Davidson C, Woodford S, Valle D, Parker G, Derias A-M, Copley C, et al. Diffuse intrinsic pontine gliomas in pediatric patients: management updates. Egyptian Journal of Neurosurgery. 2023;38(1):64.
6. Elsheikh M, Bridgman E, Lavrador JP, Lammy S, Poon MTC. Association of extent of resection and functional outcomes in diffuse low-grade glioma: systematic review & meta-analysis. Journal of Neuro-oncology. 2022;160(3):717-24.
7. Kang X-w, Xi Y-b, Liu T-t, Wang N, Zhu Y-q, Wang X-r, et al. Grading of Glioma: combined diagnostic value of amide proton transfer weighted, arterial spin labeling and diffusion weighted magnetic resonance imaging. BMC Medical Imaging. 2020;20(1):50.
8. Henriksen OM, del Mar Álvarez-Torres M, Figueiredo P, Hangel G, Keil VC, Nechifor RE, et al. High-grade glioma treatment response monitoring biomarkers: a position statement on the evidence supporting the use of advanced MRI techniques in the clinic, and the latest bench-to-bedside developments. Part 1: perfusion and diffusion techniques. Frontiers in oncology. 2022;12:810263.
9. Wang Y-L, Yao J, Chakhoyan A, Raymond C, Salamon N, Liau LM, et al. Association between tumor acidity and hypervascularity in human gliomas using pH-weighted amine chemical exchange saturation transfer echo-planar imaging and dynamic susceptibility contrast perfusion MRI at 3T. American Journal of Neuroradiology. 2019;40(6):979-86.
10. Boxerman J, Schmainda K, Weisskoff R. Relative cerebral blood volume maps corrected for contrast agent extravasation significantly correlate with glioma tumor grade, whereas uncorrected maps do not. American Journal of neuroradiology. 2006;27(4):859-67.
11. Paulson ES, Schmainda KM. Comparison of dynamic susceptibility-weighted contrast-enhanced MR methods: recommendations for measuring relative cerebral blood volume in brain tumors. Radiology. 2008;249(2):601-13.
12. Arevalo-Perez J, Peck KK, Young RJ, Holodny AI, Karimi S, Lyo JK. Dynamic contrast-enhanced perfusion MRI and diffusion-weighted imaging in grading of gliomas. Journal of Neuroimaging. 2015;25(5):792-8.
13. Ma L, Song ZJ. Differentiation between low-grade and high-grade glioma using combined diffusion tensor imaging metrics. Clinical neurology and neurosurgery. 2013;115(12):2489-95.
14. Aydin S, Fatihoğlu E, Koşar PN, Ergün E. Perfusion and permeability MRI in glioma grading. Egyptian Journal of Radiology and Nuclear Medicine. 2020;51(1):2.
15. Song D, Chen B, Li Z, Li Y, Zhao L, Wang L, et al. Role of dynamic contrast-enhanced and dynamic susceptibility contrast imaging in evaluating the biological features of glioma. Quantitative Imaging in Medicine and Surgery. 2025;15(8):7030-45.
16. Falk A, Fahlström M, Rostrup E, Berntsson S, Zetterling M, Morell A, et al. Discrimination between glioma grades II and III in suspected low-grade gliomas using dynamic contrast-enhanced and dynamic susceptibility contrast perfusion MR imaging: a histogram analysis approach. Neuroradiology. 2014;56(12):1031-8.
17. Ballato M, Germanà E, Ricciardi G, Giordano WG, Tralongo P, Buccarelli M, et al. Understanding neovascularization in glioblastoma: insights from the current literature. International Journal of Molecular Sciences. 2025;26(6):2763.
18. Guo H, Kang H, Tong H, Du X, Liu H, Tan Y, et al. Microvascular characteristics of lower-grade diffuse gliomas: investigating vessel size imaging for differentiating grades and subtypes. European radiology. 2019;29(4):1893-902.
19. Ma H, Wang Z, Xu K, Shao Z, Yang C, Xu P, et al. Three-dimensional arterial spin labeling imaging and dynamic susceptibility contrast perfusion-weighted imaging value in diagnosing glioma grade prior to surgery. Experimental and therapeutic medicine. 2017;13(6):2691-8.
20. Shin JH, Lee HK, Kwun BD, Kim J-S, Kang W, Choi CG, et al. Using relative cerebral blood flow and volume to evaluate the histopathologic grade of cerebral gliomas: preliminary results. American Journal of Roentgenology. 2002;179(3):783-9.
21. Ghodsi SM, Khoshnevisan A, Arjipour M, Ghanaati H, Firouznia K, Jalali AH, et al. Diagnostic efficacy of perfusion magnetic resonance imaging in supratentorial glioma grading. Iran J Radiol. 2018;15(2):e13696.
22. Waqar M, Lewis D, Agushi E, Gittins M, Jackson A, Coope D. Cerebral and tumoral blood flow in adult gliomas: a systematic review of results from magnetic resonance imaging. The British journal of radiology. 2021;94(1125):20201450.
23. Kaur G, Roy B. Decoding tumor angiogenesis for therapeutic advancements: mechanistic insights. Biomedicines. 2024;12(4):827.
24. Stenberg L, Englund E, Wirestam R, Siesjö P, Salford L, Larsson E-M. Dynamic susceptibility contrast-enhanced perfusion magnetic resonance (MR) imaging combined with contrast-enhanced MR imaging in the follow-up of immunogene-treated glioblastoma multiforme. Acta Radiologica. 2006;47(8):852-61.
25. Englund E. Brain Tumor Characterization Using Multibiometric Evaluation of MRI. Tomography (Ann Arbor, Mich). 2018.
26. Zakharova NE, Batalov AI, Pogosbekian EL, Chekhonin IV, Goryaynov SA, Bykanov AE, et al. Perifocal zone of brain gliomas: application of diffusion kurtosis and perfusion MRI values for tumor invasion border determination. Cancers. 2023;15(10):2760.
27. Varakis L, Rologis D, Grivas A, Vretakos G, Papanikolaou N, editors. Pearls and pitfalls of physiology based MR imaging in brain tumors2010: European Congress of Radiology-ECR 2010.
28. Chelebian E, Fuster-Garcia E, Álvarez-Torres MdM, Juan-Albarracín J, Garcia-Gomez JM. Higher vascularity at infiltrated peripheral edema

differentiates proneural glioblastoma subtype. PLoS One. 2020;15(10):e0232500.
29. Senturk S, Oguz KK, Cila A. Dynamic contrast-enhanced susceptibility-weighted perfusion imaging of intracranial tumors: a study using a 3T MR scanner. Diagn Interv Radiol. 2009;15(1):3-12.
30. Pries AR, Höpfner M, Le Noble F, Dewhirst MW, Secomb TW. The shunt problem: control of functional shunting in normal and tumour vasculature. Nature Reviews Cancer. 2010;10(8):587-93.